# STATISTICAL DOWNSCALING OF MODIS THERMAL IMAGERY TO LANDSAT 5 TM+ RESOLUTIONS

J. Jeremy Webber III

Submitted to the faculty of the University Graduate School
in partial fulfillment of the requirements
for the degree
Master of Science
in the Department of Geography,
Indiana University
August 2013

Accepted by the Faculty of Indiana University, in partial fulfillment of the requirements for the degree of Master of Science.

Daniel P. Johnson Ph.D

Jeffrey S. Wilson Ph.D

Master's Thesis
Committee

Owen J. Dwyer Ph.D

ACKNOWLEDGEMENTS

I thank my graduate advisor, Dr. Daniel P. Johnson for providing me an opportunity to earn a Master of Science under his guidance. Dr. Johnson has been a thoughtful and considerate mentor throughout my graduate career. I am thankful to the National Aeronautical Space Administration (NASA) Research Opportunities in Space and Earth Sciences (ROSES) program for funding this work (grant no. 439-2078). It is a pleasure to work with our colleagues in the ROSES program. Their interests and enthusiasm for our work was motivational to me.

I am grateful to Dr. Jeffery Wilson and Dr. Owen J. Dwyer for serving on my thesis committee. Both are accomplished Faculty Members and each brings a unique perspective to my research. I owe much gratitude to my laboratory partner, Dr. Vijay Lulla. Dr. Lulla was instrumental in getting me to look at my research from different perspectives. I appreciate his patients and willingness to discuss my research with me.

While working on my thesis two of my close friends would frequently be in contact. I began to see a pattern. After general pleasantries, I would anticipate their reoccurring questions: “Where are you at with your thesis work?” or, “Have your tuned in your thesis yet?” It comes from a good place and I thank Jerry Paar and Eric Simpson for caring enough to ask.

I appreciate my Mother and Father for listening to me throughout the graduate process. I appreciate my Father’s technical advice while doing this work. His background in electrical engineering overlaps with my remote sensing work. It was fun to discuss my research problems with him.

Lastly and certainly not least, I would like to thank Brandy L. Kinser for staying by me throughout my education. I appreciate her support in many ways.

TABLE OF CONTENTS

LIST OF TABLES

LIST OF FIGURES

LIST OF ABBERVIATIONS

°C: Degrees Celsius
°F: Degrees Fahrenheit
ALI: Advanced Land Imager
AOI: Area of Interest
ASTER: Advanced Spaceborne Thermal Emission and Reflection Radiometer
CBD: Central Business District
CDC: Centers for Disease Control
CFC: Chlorofluorocarbons
$CH_4$: Methane
$CO_2$: Carbon Dioxide
DEM: Digital Elevation Model
DN: Digital Number
EHE: Extreme Heat Events
EHVI: Enhanced Heat Vulnerability Index
EPA: Environmental Protection Agency
EROS: Environmental Resources Observation and Science Center
ETM+: Enhanced Thematic Mapper Plus
GCP: Ground Control Points
GCS: Geographic Coordinate System
GHG: Greenhouse Gasses
$H_2O$: Water Vapor
HDF: Hierarchical Data Format
IPCC: Intergovernmental Panel on Climate Change
KM: Kilometer
LST: Land Surface Temperature
MCHD: Marion County Health Department
MODIS: Moderate Resolution Imaging Spectroradiometer Sensor
MSS: Multispectral Scanner System
$N_2O$: Nitrous Oxide
NASA: National Aeronautics and Space Administration,
NWS: National Weather Service
$O_3$: Ozone
PCA: Principal Components Analysis
PPB: Part Per Billion
PPM: Part Per Million
RMSE: Root Mean Squared Error
SAR: Synthetic Aperture Radar
TIFF: Tagged Image File Format
TIR: Thermal Infrared
TM: Thematic Mapper
TOA: Top of Atmosphere
UHI: Urban Heat Islands
USGS: United States Geological Survey
UTM: Universal Transverse Mercator
WGS: World Geodetic System

## Introduction

The basis of this thesis is to emulate a sensor that can predict a downscaled daily Land Surface Temperature (LST). If error is minimal, downscaled daily LSTs can be incorporated with risk assessment models enabling the ability to monitor and predict risk during an extreme heat event. Imagery with high spatial resolutions are needed in order to monitor intra-urban variations of LSTs. Several platforms exist such as Landsat 7 TM+ / ETM+ and ASTER (120 M / 60 M and 90 M), but these sensors lack the temporal resolution needed to calibrate vulnerability models on a daily basis (Johnson, Lulla, Stanforth, and Webber, 2011). The Moderate Resolution Imaging Spectroradiometer (MODIS) sensor platform has a temporal resolution of twice daily, but lacks the spatial resolution (1 KM) needed to monitor micro heat climates within urban areas.

The method presented in this thesis will test the possibility to emulate such a sensor needed to meet these criteria by applying multisensory data fusion techniques to different spatial and temporal resolution sensors (Johnson et al., 2011). Coupling the higher spatial resolution thermal band from Landsat 5 TM+ with the twice daily acquisition from the MODIS platform could prove beneficial in predicting the oncoming day(s) LST (Johnson et al., 2011). This will be accomplished by utilizing matrix based analysis techniques that correspond with variations of the Landsat 5 TM+ image within the MODIS image pixel (Johnson et al., 2011). This allows for the opportunity to create an image that has both the spatial and temporal resolution needed to extrapolate a daily downscaled LST. This image fusion technique will be tested and re-calibrated after every cloud free Landsat 5 TM+ pass (Johnson et al., 2011).

## Literature Review

### Background

Current literature and climatic models suggest that extreme heat events will be more frequent and intense in the future (Johnson, Wilson, and Luber, 2009). Heat waves in context with other natural disasters are responsible for the most weather related fatalities in the United States. Heat-related health risk have not been thoroughly investigated in a geospatial framework to the extent of other natural disasters (e.g. hurricanes, tornados, flooding, and wildfires) (Johnson et al., 2011). Heat waves are responsible for more deaths in North America than hurricanes, lightning, and tornados combined (Pengelly, Campbell, Cheng, Fu, Gingrich, and Macfarlane, 2007). Heat-related mortality and morbidity usually occur in the summer months, and many of these deaths can be prevented (CDC, MMWR July 27, 2001). The Centers for Disease Control (CDC) report that there are approximately 400 deaths attributed to excessive natural heat each year (MMWR, July 5, 2002). As global average temperatures continue to increase Extreme Heat Events (EHEs) will remain an issue in the United States. Governmental agencies such as the National Aeronautical and Space Administration (NASA), the Centers for Disease Control (CDC), Environmental Protection Agency (EPA), and local Health Departments of the cities that are most vulnerable to extreme heat are concerned about future heat-related health risk associated with EHEs. The Excessive Heat Events Guidebook published by the EPA and other contributing agencies state that "EHEs may become more frequent, more severe, or both in the United States" (2006).

Heat-related deaths and illness are preventable, but there is an overall lack of recognition by the public that extreme heat is in fact dangerous (Luber and Mc Geehin, 2008). Unlike other natural disasters excessive heat is a silent killer (Luber and Mc Geehin, 2008). When periods of heat subside, and cooler weather returns, the perception of heat-related

illness fades unlike the devastation that is left behind in the wake of tornados, hurricanes, or flooding (Johnson et al., 2011).

Increasing awareness of EHEs is necessary as adverse effects of extreme heat can usually be mitigated reducing morbidity and mortality (EPA, 2006). The responsibility for early detection and warning response falls within the hands of first responders, meteorological data molders, and academic researchers (Johnson et al., 2011). The vulnerable portions of the population that are most susceptible to EHEs are older persons (age > 65), Infants ( age < 1), homeless, poor, people who are socially isolated, those with mobility or mental impairments, those who take specific kinds of medication that can inhibit a person's thermoregulatory system (e. g. antihistamines, blood pressure medication), those that exercise or work outdoors, and those who work outdoors under the influence of drugs or alcohol (EPA, 2006; Cutter, Boruff, and Shirley, 2003). Although the dangers of EHEs can be averted; there is a general lack of perceived risk associated with heat waves.

Over exposure during extreme heat conditions places stress on the body's natural ability to maintain its ideal internal temperature of 98.6 °F, which is critical for normal physical functioning (CDC, 2004). The most common heat-related-illnesses stem from prolonged exposure to excessive heat. The most common symptoms of heat-related illness are heat cramps, heat syncope, heat exhaustion, heat stroke, and in the most severe cases, death (Luber and Mc Geehin, 2008). Signs of heat-related illness include but are not limited to painful muscle cramps, heavy sweating, weakness, dizziness, fainting, nausea, an altered mental state, headache, and confusion (CDC, 2004; Luber and Mc Geehin, 2008).

For the first half of the 21st century climate models are projecting expected year round temperatures to warm approximately 1 to 3 °C across North America (Johnson and Wilson, 2009; Alley, Berntsen, Bindoff, Chen, Chidthaisong, et al., 2007). There have been notable

changes in extreme temperatures over the last 50 years. The Intergovernmental Panel on Climate Change (IPCC) reported in its *Fourth Assessment Report, Summary for Policy Makers* that "cold days, cold nights, and frost have become less frequent, while hot days and hot nights have become more frequent" (Alley et al., 2007). Surface temperatures are rarely uniform across the urban environment and the lack the nighttime cooling during extend periods of hot weather can place those that might not be considered as vulnerable at greater risk of heat-related morbidity or mortality as EHE conditions persist.

Coupling socioeconomic indicators with LSTs at the Census Block Group and Tract Level has enabled us to develop models that more precisely locate the areas and people most vulnerable to an EHE within the urban environment. Using remotely sensed data enables better evaluation of LSTs across a continuous surface in the urban environment. LSTs increase the robustness of risk assessment models currently being developed by our team.

Principal Components Analysis (PCA) was used in our previous work to model vulnerability to extreme heat. Cakir and Khorram define PCA as one of the most widely used data fusion approaches used with remote sensor data (2008). They broadly define PCA as "a multivariate statistical technique that deals with the internal structures of matrices" (Cakir and Kohorram, 2008). They further describe that PCA "breaks down or partitions a resemblance matrix into a set of orthogonal (perpendicular) axes or components" (Cakir and Kohorram, 2008). The output matrix usually consists of variance-covariance, or correlations (Cakir and Kohorram, 2008). A correlation matrix was used in our previous models which is known as factor analysis (Cakir and Kohorram, 2008). With factor analysis "each PCA axis corresponds to an eigenvalue of the matrix" (Cakir and Kohorram, 2008). These types of data driven models will be useful for first responders by allowing increased time for planning, and by knowing where to

better allocate resources during extreme heat events. The objective in developing these vulnerability models is to help reduce heat-related morbidity and mortality.

In order to advance this work, and to fulfill the requirements for Masters of Science in Geographic Information Science, the objective of this thesis is to develop a data fusion method to apply to different spatial and temporal resolution satellite images in order to predict the oncoming days' LST values. By downscaling mean LST values and combining these fused images with socioeconomic and demographic data it may be possible to model vulnerability on a daily basis during a heat wave. These data could be combined with meteorological forecasts for an area to predict Urban Heat Island (UHI) intensity (Johnson et al., 2011). If this remote sensing calibration study is successful these data would be hugely important to first responders by allowing increased time for mitigation and intervention planning (Johnson et al., 2011). Such information would also aid in planning the distribution of cooling and hydration centers.

**A Changing Climate**

The Earth's weather and climate is dynamic to say the least, and has varied naturally through time shifting between glacial and interglacial periods for millennia. Anthropogenic actives, especially since the pre-industrial era have brought about "changes in the atmospheric abundance of greenhouse gasses and aerosols, [changes] in solar radiation and in land surface properties [that] alter the energy balance of the climate system" (Alley et al., 2007). This section will differentiate between the natural greenhouse effect and enhanced greenhouse effect, define the atmospheres most important heat-trapping gasses, and describe how a changing climate will increase the intensity and areal extent of heat waves in the future.

**Greenhouse Effect versus Radiative Forcing**

It is important to understand the difference between the natural and enhanced greenhouse effect. There is a natural abundance of ozone in the lower stratosphere. These

molecules “absorb heat radiated from Earth’s surface in the lower atmosphere and then radiate much of that energy back towards the surface” (Karl et al., 2009). Without this natural greenhouse effect Earth would be approximately 60 °F cooler (Karl et al., 2009). However, additional human activities have released an abundance of heat-trapping gasses over the last approximate 260 years (Karl et al., 2009). The addition of these Greenhouse Gasses (GHG) has intensified the natural greenhouse effect, which in turn changes the Earth’s climate (Karl et al., 2009). When looking at the global concentrations of GHGs from ice core data covering the span of the last 800,000 years it is evident that human actives have contributed to the increase of global GHG concentrations (Alley et al., 2007). To what degree is not the objective of this paper. For more information regarding this topic refer to the publications put forth by the Intergovernmental Panel on Climate Change (IPCC) or the U.S. Global Change Research Program.

The most important heat-trapping gasses in the Earth’s atmosphere are: carbon dioxide ($CO_2$), methane ($CH_4$), and nitrous oxide ($N_2O$), halocarbons, ozone ($O_3$), and water vapor ($H_2O$). These molecules absorb and radiate heat at different rates. The most important GHG is carbon dioxide (Alley et al., 2007) and the concentration has largely increased due to the burning of fossil fuels for electric generation, transportation, and industrial and household uses (Karl et al., 2009). The pre-industrial global concentrations of carbon dioxide were approximately 280 Parts Per Million (PPM) and has increased to 379 PPM (2005 concentration) (Alley et al., 2007). Over the last century “about 80% of human-induced carbon dioxide emissions came from burning fossil fuels, while about 20% resulted from deforestation and associated agricultural practices” (Karl et al., 2009).

Methane is an important GHG and should not be overlooked. While methane is not as abundant by total percent composition when compared to other GHGs in the atmosphere it has a large heating potential in the lower atmosphere. The increase in the concentration of

methane is primarily due to the raising of livestock which pass methane through their digestive system. Other anthropogenic activities such as, "mining and transportation, sewage and decomposing landfills are other anthropogenic sources of methane" (Karl et al., 2009). It is reported that approximately 70% of the methane in Earth's atmosphere is due to anthropogenic activity (Karl et al., 2009). The pre-industrial global atmospheric concentrations of methane were approximately 715 Parts Per Billion (PPB) and have increased to 1774 PPB (2005 concentration) (Alley et al., 2007).

Another important GHG is Nitrous oxide which has increased as a result of being used as fertilizer and for fossil fuel burning. The pre-industrial global atmospheric concentrations of nitrous oxide have increased from 270 ppb to 319 (2005) (Alley et al., 2007). A smaller but still harmful GHG agent is halocarbons. Halocarbons are released from certain manufactured chemicals (Karl et al., 2009). A type of halocarbon is chlorofluorocarbons (CFCs). CFCs were abundantly used in refrigerant and other industrial applications, but were found to be depleting the ozonosphere and were banned (Karl et al., 2009). The abundance of halocarbons is expected to continue to decline, however many halocarbon replacements contain potent GHGs, and atmospheric concentrations of these gases are increasing (Karl et al., 2009).

Water vapor is the most abundant greenhouse gas by percent composition of the atmosphere, and is also the most important GHG due to the significance that it has in moderating weather and climate (Karl et al., 2009). Human activities do not necessarily increase water vapor through irrigation and combustion processes, although the other GHGs released by human activity have warmed surface temperatures allowing the air to hold more moisture (Karl et al., 2009). The average water vapor content in the atmosphere has increased since the 1980s over land, ocean, and in the upper troposphere (Alley et al., 2007).

Human activities also produce local and regional effects (Karl et al., 2009). The changes in surface materials can "alter how much heat is reflected or absorbed" (Karl et al., 2009). The most obvious changes are "the cutting and burning of forest, and the replacement of areas of natural vegetation with agriculture with large scale irrigation" (Karl et al., 2009).

Much like the rest of the world, the U.S. has been warming significantly over the last 50 years (Karl et al., 2009). Temperature increases over the next few decades will largely be determined by past emissions of GHGs (Karl et al., 2009). For most of the U.S. temperatures will be warmer in the summer (Karl et al., 2009). By the end of the century climate models are projecting a best case scenario of temperatures rising by 4 to 6.5 °F and a worst case scenario of temperatures rising by approximately 7 to 11 °F (Karl et al., 2009 and Alley et al., 2007). Neither scenario should be ignored as these temperature modifications are likely to produce weather extremes.

With respect to extreme heat, the U.S. has experienced more "unusually hot days and nights fewer unusually cold days and nights, and fewer frost days" over the last few decades (Karl et al., 2009 and Alley et al., 2007). A key defining component amongst the published definitions for high humidity heat waves are that they range in time period from a few days to a few weeks. Over the last three to four decades there has been an increasing trend in high humidity heat waves, "which are characterized by the persistence of extremely high nighttime temperatures" (Karl et al., 2009). With the current climatic patterns the U.S. can expect "average temperatures to rise throughout this century, the frequency of cold extremes will decrease, and the intensity and frequency of high temperature extremes will increase" (Karl et al., 2009). Through recent studies an "ensemble of models" indicates that EHE events which are considered rare by today's standards (occurring once every 20 years) will occur every other year in the U.S. by the end of the century (Karl et al., 2009).

The CDC reports that during an average summer approximately 400 American mortalities are related to extreme heat (Stone, Hess, and Frumkin, 2010; Bernard and McGeehin, 2004). Listed below are a few of the most notable extreme heat events in the recent past. The 1995 heat wave of Chicago killed more than 700 people in a five day period (EPA, 2006). The 2003 European heat wave is estimated to have killed over 70,000 people in a few months (Stone et al., 2010). 117 mortalities were recorded in Philadelphia over a seven day period in 1995 (Johnson and Wilson, 2009). The threat of extreme heat is real, and should be considered as Earth's climate continues to trend in a warmer direction.

**Heat Waves Defined**

There is not a universal definition that fully describes an EHE across climatic regions and through time. This section will review contemporary definitions of heat waves as well as further describe the characteristics and determining factors associated with extreme heat. According to the Excessive Heat Events Guidebook extreme heat events are "defined by summertime weather that is substantially hotter and / or more humid than average for a location at that time of year" (EPA, 2006). This definition has broad applicability by not getting over detailed about minimum, maximums, or relative humidity values. A basic, but well thought out definition of extreme heat has been defined by Robinson: "A heat wave implies that it is an extended period of unusually high atmosphere-related heat stress, which causes temporary modifications in lifestyle and which may have adverse consequences for the affected population" (2000).

Another complicating factor in defining a heat wave is the different nomenclature that is used across the United States (Johnson, 2009). For example the California Energy Commission calls a heat wave a heat storm (Johnson, 2009). The National Weather Service (NWS) has created a "de facto basic heat wave definition" for the purposes of issuing heat alerts and warnings (Robinson, 2000). These criteria have nationwide standards and allow for deviations

based on local climate conditions (Robinson, 2000). How hot it actually feels depends on the interaction of several meteorological variables such as temperature, humidity, and cloud cover (EPA, 2006).

The NWS issues Excessive Heat Outlooks, Excessive Heat Watches, and Excessive Heat Warnings / Advisories which are based on heat index temperatures (NWS, 2011). Excessive Heat Outlooks are issued when there is the potential for extreme heat within the next three to seven days (NWS, 2011); giving first responders a chance to prepare for an extreme heat event (NWS, 2011). Excessive Heat Watches are issued when conditions are favorable for extreme heat within the next 24 to 48 hours (NWS, 2011). Watches are issued when there is still uncertainly as to when the EHE will occur (NWS, 2011). Excessive Heat Warnings / Advisories are issued when extreme heat "is imminent, or has a very high probability of occurring within the next 36 hours" (NWS, 2011). The NWS states that "warning[s] [are] used for conditions that pose a threat to life or property" and "advisories [are] for less serious conditions that cause significant discomfort or inconvenience and, if caution is not taken, could lead to a threat to life and / or property" (2011). The NWS issues alert procedures "when the Heat Index is expected to exceed 105° - 110 °F (depending on local climate) for at least two consecutive days" (NWS, 2011).

It is also important to take into account that "EHE criteria typically shift by location and time of year" (EPA, 2006). Cities such as Dayton, Indianapolis, Philadelphia, and Phoenix are "likely to have different EHE criteria at any point in the summer to reflect different local standards for unusually hot summertime weather" (EPA, 2006). The Excessive Heat Events Guidebook also notes that EHE conditions are likely to change for each city over the summer and as a result this inhibits the ability to have absolute criteria that defines the constituents of an EHE through time and place (2006).

**Urban Heat Islands**

Understanding urban heat islands is central to modeling vulnerability to extreme heat. The characteristics of the built environment in conjunction with anthropogenic activities associated with cities make it more likely that urban environments will be hotter during an EHE. Approximately half of the world's population lives in urban areas making it hugely important to understand the microclimates of the built environment. This section will describe this phenomenon; specifically how modeling a daily downscaled LST could help monitor changes in urban microclimates. If warm air in an area remains stagnate and extreme heat persist the general premise is that these areas continue to warm exacerbating the next day(s) extreme temperatures. Increasing the resolution at which thermal data are observed across a continuous surface could enable extreme heat vulnerability to be modeled on a daily basis.

According to the Excessive Heat Events Guidebook an urban heat island is a phenomenon where an urban area is considerably warmer than the surrounding areas (EPA, 2006). The temperature differential between urban and rural areas can be as much as 10 °F and result from several factors such as: loss of vegetation which accompanies loss of evapotranspiration; dark surfaces which lower albedo, which in turn absorbs and reradiates heat; building configurations which trap heat and can restrict air flow; and concentrated heat producers such as generators and cars (Stone et al., 2010). A UHI is commonly characterized by high population density and characteristics from the built environment that contribute to localized increases in surface temperatures. This creates a micro-climatic condition that is influenced by modifications in land use patterns caused by built-up features and the heat storing capacity of building materials, lack of vegetation, and heat generated from energy usage (EPA, 2006).

The Excessive Heat Events Guidebook states that "regional characteristics can help determine individual's health risks during an EHE" (EPA, 2006). These factors include geographic location, urbanization and urban design, and residential location. While "climate variability is largely a function of location" (EPA, 2006), the spatiality is not as clear-cut as it may seem. For example Phoenix is regionally warmer than Dayton or Philadelphia, but that does not necessarily mean that Phoenix would be the most at risk to EHE solely because of their geographic location.

Urbanization and urban design play a large role in attenuating LST values. It is important to mention that cities have been decentralizing over the past decades in a phenomenon known as urban sprawl (Stone et al., 2011). Buildings with dark roofs and dark surface materials tend to replace vegetation in cities as they sprawl. This changes the latent heat storage capacities at the surface, which in turn contributes to creating discontinuous microclimates that can be distinctively different than the surrounding environment.

The presence or lack of vegetation can strongly influence LSTs. Areas with a dense tree canopy can experience much cooler temperatures then areas largely constructed with manmade materials. Lack of vegetative cover and replacement with non-natural materials that have a lower albedo can increase LST values dramatically. Building materials and construction style also play a large role in contributing to an increase in LST values. Philadelphia has many old solid brick structures with flat-top black roofs. Historically Philadelphia was built to withstand cold winters. These characteristics contribute to warming the structure making it more difficult to cool during the summer months. These solid structure buildings made of either brick or stone have high heat retention capacities which strongly contribute to enhanced LSTs in the surrounding environment as well. It is also worth mentioning that older buildings such as those in the city of Philadelphia have not been retrofitted for central air. In some cases residential dwellings may not have central air or a window unit, and depending on the safety of

the neighborhood residents might not even open their windows due to safety concerns. The Philadelphia Center for Aging reports that residents in troubled neighborhoods have nailed their windows shut for security measures (EHE Focus Group Meeting, 2010).

Another contributing factor that is not often thought about in the context of extreme heat is residential location and urban density. The adiabatic process states that as air becomes warmer it rises. As air rises to higher altitudes it cools, condenses, and falls back to the surface completing a convection cycle. Those that live in a multilevel or a high rise building can expect to feel warmer inside temperatures due to the convective nature of warm air. The presence of large buildings, especially in the Central Business District (CBD) or industrial areas of cities can restrict air flow. This can make it more difficult to maintain a consistent internal temperature, especially if air conditioning is not available or used, or if ventilation is restricted (EPA, 2006).

**Perception of Extreme Heat Events**

Although there are high mortality rates associated with EHE conditions, and projections of a warmer climate, there is still a general lack of recognition by the public that extreme heat exposure is a problem and will continue to be in the future (Luber and Mc Geehin, 2008). Many U.S. metropolitan areas generally lack preparedness measures such as heat wave-response plans (Luber and Mc Geehin, 2008). Heat waves are silent killers and do not leave a wake of visible destruction like other natural disasters (Johnson, 2009; Luber and Mc Geehin, 2008). The success of public health efforts to reduce morbidity and mortality during an EHE "hinges on their ability to effect behavior change in individuals during these events" (Luber and Mc Geehin, 2008). Despite the lethal nature of extreme heat the public lacks the recognition of the lethality of these events, and "many at-risk individuals are unaware, or unwilling to take appropriate preventative measures" (Luber and Mc Geehin, 2008).

Although an individual may take preventative measures the first few days of an EHE the perception of the threat from extreme heat diminishes as hot conditions persists (Luber and Mc Geehin, 2008). In order to examine the efficiency of heat watch / warning systems Sheridan investigated heat mitigation plans across four North American cities paying specific attention to people's perception of their vulnerability to extreme heat (2006). As well as gauging perception, Sheridan also assessed people's knowledge of heat warning systems and the measures to help mitigate extreme heat (2006). After conducting a 980 person telephone survey Sheridan found that the vast majority (90%) was well aware of the warning systems due to pervasive media coverage, but respondents were less familiar with what to do during an EHE (2006). Sheridan mentions that since the 1995 heat wave in North America (specifically the Chicago area) there has been an increased interest in modeling heat vulnerability, but a paucity of literature dealing with how people "perceive their own vulnerability and their options for dealing with extreme heat" (2006).

According to Bernard and Mc Gheein, many cities across North American have minimal or no heat wave plans at all (2004). In the summer of 2002 they reviewed preparedness plans for eighteen cities that are at risk of EHE and that have had historic mortality related to heat events (Bernard et al., 2004). Their objective was to determine if the response plans "reflected awareness of the risk, risk factors, and response measures" and their findings suggest that this topic should be an important "area of future investigation and government attention" (Bernard et al., 2004). From their study they found that a third of the eighteen cities surveyed lacked response plans and of the ten cities that had response plans one third are superficial (Bernard et al., 2004). Developing comprehensive heat response plans requires collaboration amongst city government and nongovernmental organizations (Bernard et al., 2004). In many cities throughout North America the public health department facilitates communication between

these entities to develop heat response plans. Most of the review plans reviewed by Bernard et al. indicate that "heat response was coordinated by public safety or emergency management offices, but few were based in the public health department" (2004).

Bernard et al. mention several other interesting observations regarding their assessment of eighteen city heat wave response plans (2004). It is interesting to note that "a few plans took a phased approach to response, which is valuable because mortality increases nonlinearly with the duration of the heat wave" (Bernard et al., 2004). This is a progressive approach to dealing with extreme heat through time as more mortality can be expected if the intensity of a heat wave persists for an extended period of time. In an attempt to make centralized cooling available during EHE conditions those who do not have air-conditioning, or cannot afford air-conditioning, have the option in many cities to visit a cooling center (Bernard et al., 2004).

Cooling centers are used as a resource to mitigate adverse reactions to extreme heat on the vulnerable portions of the population. In theory cooling centers should be at capacity during an EHE, but that does not appear to be the case in some North American cities. During the 2011 EHE in Indianapolis the Marion County Health Department (MCHD) reported that attendance was overall low at the eight cooling centers, which were located in the hottest and most vulnerable portions of the city (Marion County Health Department, Personal Communication by Daniel P. Johnson, 2011). Comments posted by Indianapolis citizens on a heat-related article written by local news station WTHR13, indicated that placing cooling centers mostly in areas of high vulnerability might not be sufficient. People commented that that most of the cooling centers seemed to be placed in the poorest areas of the city and stated that even though they were not below poverty their air conditioners could not keep their houses sufficiently cool during the EHE, and they would have liked a cooling center located closer to

their neighborhood (WTHR13, 2011). This information might be helpful for the placement of future summers' cooling centers.

Another mitigation program widely used across cities in North America is fan distribution. Of the eighteen response plans reviewed "five cities reported having fan distribution programs despite evidence that fans do not reduce mortality during heat waves and can increase heat stress if used improperly" (Bernard et al., 2004). If fans are used when the heat index exceeds 99 °F they can increase heat stress on the body due to the effect of blowing air on the skin that is warmer than the body (Luber and Mc Geehin, 2008). The problem that arises from fan distribution programs is that residents may operate fans improperly by not opening their windows, further exacerbating heat-health risk associated with extreme heat.

**Current Literature Pertaining to Fusing Images of Different Spatial and Temporal Resolutions**

The wide range of remotely sensed data available at low cost or even free has enabled scientists to develop many published image fusion techniques. Simone et al. broadly define image fusion as "the acquisition, processing, and synergistic combination of information provided by various sensors or by the same sensor in many measuring contexts" (2002). Digital image fusion is the science of combining different images in order to obtain more inferences than can be obtained from a single sensor (Dong et al., 2009). In this process images of different resolution (spatial, spectral, and radiometric) are combined to form a composite image making "it easier for the user to detect, recognize, and identify targets and increase situational awareness" (Dong et al., 2009).

The objective of this thesis is to downscale higher spatial resolution thermal imagery (Landsat 5 TM+) in an attempt to increase the spatial resolution of thermal bands from the lower spatial resolution thermal imagery (MODIS). A weighted matrix is created in order to predict daily LST values by using information from two sensors that have different spatial and

temporal resolution. This section reviews multisensory data fusion techniques in order to assess potential methods to support this thesis. Of the hundreds of variations of image fusion available only those that seem most applicable to this study will be reviewed.

Simone et al. describes three typical applications of data fusion; one of which is applicable to this study. These authors have surveyed different methods of image fusion for multi-temporal / multi-sensor remotely sensed images of the same location, but with different dates (2002). In their study they experimented with various techniques of fusing images from the Synthetic Aperture Radar (SAR) sensor and Landsat 7 ETM+. There are several methodologies that have been proposed for the purpose of multi-sensor fusion and are "based on statistical, symbolic, and neural-network approaches" (Simone et al., 2002). In their work they identified the neural-network approach as "providing an effective integration of different types of data," and "the non-parametric approach allows the aggregation of different data sources into a stacked vector without the need for assuming a specific probabilistic distribution of the data to be fused" (Simone et al., 2002). In working with Professor Johnson we have developed a statistical model to fuse the images of interests together. Statistical downscaling will be applied to Indianapolis, IN. In this study and error will be evaluated between actual and modeled temperatures. More detail of this is provided in the Methodology and Results sections.

## Methodology

### Statistical Downscaling of MODIS Thermal Imagery to Landsat 5 TM+ Resolutions

The specific objective of this study is to develop a weighted temperature matrix from Landsat 5 TM+ to calibrate daily MODIS MOD11A1 Terra LST values. The result would be a composite image of daily LST values. With the MODIS MOD11A1 sensor passing twice daily and Landsat 5 TM+ every sixteen days, the higher resolution Landsat 5 TM+ image will be used to weight the daily MODIS MOD11A1 LST values in order to get a downscaled LST for the upcoming day. The weighted temperature matrix is based on the temperature delta between MODIS MOD11A1 and Landsat 5 TM+. What is essentially being accomplished is a downscaling of MODIS MOD11A1 thermal imagery with higher resolution thermal data from the Landsat 5 TM+ sensor. The daily MODIS MOD11A1 thermal image represents the observed value and the Landsat 5 TM+ thermal imagery is being used as a means to downscale the LST values of the MODIS MOD11A1 imagery. Downscaling is accomplished by calculating the differences between the daily observed LST from MODIS MOD11A1 with the higher resolution LST value from Landsat 5 TM+ (Figure 1). The hypothesis is that the sum of MODIS MOD11A1 LST values will approximate the sum of Landsat 5 TM+ LST values.

In the downscaling equation (Figure 1) the MODIS MOD11A1 mean LST approximates the sum of Landsat 5 TM+ mean LST values applied across the MODIS matrix. The key component in this equation is the calculation of the weighted LST value. To approximate a downscaled temperature Landsat 5 TM+ is subtracted from MODIS MOD11A1 on day one. This is the initial downscale calibration from both sensors. On day two the output from day one is then added to each subsequent day. Figure 1 represents one MODIS MOD11A1 pixel with a LST value of 96 °F and the most recent Landsat 5 TM+ LST value of 100 °F in the region of the top left corner of the MODIS MOD11A1 pixel. This calculation computes the temperature difference (in

this case of 4 °F) and changes the value for that pixel to a value of 100 °F. The downscaling calculation is applied across the MODIS MOD11A1 matrix by using the Model Builder in ERDAS Imagine 9.3. MODIS MOD11A1 LST values are downscaled using the method mentioned above and will then be compared to the observed LST values of the next cloud free Landsat 5 TM+ image. The Root Mean Squared Error (RMSE) test will be used to measure error between the daily downscaled composite (predicted) and the next cloud free Landsat 5 TM+ image.

For every daily MODIS MOD11A1 pass the most recent cloud free Landsat 5 TM+ weight will be calculated and downscaled to enhance the spatial resolution of the MODIS MOD11A1 image. The weighted matrix is to be re-calibrated after the next cloud free Landsat 5 TM+ pass (usually 16 days).

**Study Area**

This thesis will apply statistical downscaling methods in Indianapolis, IN. Statistical downscaling methods will be tested during the July 2011 extreme heat event, which had high heat index values, and persisted for several days across the Midwest. Indianapolis was under extreme heat watches, warnings, or advisories during the time period of this study; 2011-07-15 to 2011-07-31.

**Remote Sensor Data**

This research utilizes thermal imagery from Landsat 5 TM+ and the MODIS Terra sensor. These data have very different characteristics when compared to one another. This study utilizes thermal imagery from two NASA satellites (Table 1) that have different spatial and temporal resolutions. The intent of this study is to utilize the different spatiotemporal characteristics from each sensor to generate a composite image that will create thermal information that otherwise could not be obtained on a daily basis at a higher resolution. Imagery from both sensors are georectified by NASA using Ground Control Points (GCP) and

RMSE values are published in the metadata for each image. Imagery for this study was obtained from GloVis USGS Global Earth Resources Observation and Science Center (EROS).

**Landsat 5 TM+ Thematic Mapper**

Landsat 5 TM+ collects a top of atmosphere (TOA) radiance, which needs further processing to be converted to a LST value. This will be explained in the Thermal Image Processing section. The Landsat 5 TM+ sensor collects Thermal Infrared (TIR) data in Band 6 (10.40μ - 12.50μ) every sixteen days with a spatial resolution measuring 120 M x 120 M (USGS, 2011). Landsat 5 TM+ TIR data are re-sampled and smoothed in post processing to higher spatial resolutions. It is important to note that Landsat 5 TM+ Band 6 imagery acquired before February 25, 2010 is re-sampled from 120-meter pixels to 60-meter pixels (USGS, 2011). Imagery collected after February 25, 2010 is re-sampled from 120-meter pixels to 30-meter pixels. The Landsat 5 TM+ sensor has an 8-bit radiometric resolution (USGS, 2011). The Landsat 5 TM+ sensor passes over Indianapolis, IN in the mid-afternoon. Landsat 5 TM+ scene center scan times for Indianapolis are approximately 4:12 p.m. (Landsat 5 TM+ Metadata).

This study utilizes Level 1T (terrain correct) Landsat 5 TM+ Imagery. Level 1T processing "provides systematic radiometric and geometric accuracy by incorporating ground control points, while also employing a Digital Elevation Model for topographic accuracy" (USGS, 2009). Landsat 5 TM+ is projected in World Geodetic System (WGS) 1984 Universal Transverse Mercator (UTM+) Zone 16 for Indianapolis.

**Moderate Resolution Imaging Spectroradiometer (MODIS) Terra**

This study utilizes MODIS Terra V005 MOD11A1 LST (1 KM) science data set layers (LP DACC, 2012). These data are validated through field campaigns and are ready for scientific use (LP DACC, 2012). MODIS collects a twice daily LST product (Earth Resources Observation Center,

2011). The MODIS MOD11A1 sensor collects TIR data in Band 31 (10.780µ - 11.280µ) and Band 32 (11.770µ - 12.270µ) twice daily (day and night) with a spatial resolution measuring 1 KM x 1 KM (Earth Resources Observation Center, 2011). The MODIS MOD11A1 TIR sensors have a 16-bit unsigned radiometric resolution (Earth Resources Observation Center, 2011).

Although MODIS sensors collect moderate spatial resolution imagery, the temporal resolution of this imagery is prime for fusing with other satellite imagery that has a greater spatial resolution but less temporal coverage. According to NASA "The MODIS instruments on board Terra and Aqua Satellites acquire data continually providing global coverage every 1-2 days" (NASA, 2012). The MODIS sensors are polar-orbiting spacecraft, and "are synchronized with the sun in order to pass over the same area at the same time every day" (NASA, 2012). The MODIS "satellites orbit the Earth once every 99 minutes at an inclination of 98 degrees relative to the equator, at a mean altitude of 438 nautical miles" (NASA, 2012) The Terra sensor is used in this study and crosses the equator at 10:30 a.m. local time (NASA, 2012).

**Data Preparation**

Landsat 5 TM+ and MODIS MOD11A1 are delivered in different formats and geoprocessing functions must be performed before analysis can take place. MODIS MOD11A1 is delivered in Hierarchical Data Format (HDF). Once uncompressed MODIS MOD11A1 data are ready for viewing in geospatial software that allows the HDF file extension. The post processed Landsat 5 TM+ data are delivered as individual bands in the Tagged Image File Format (TIFF). Landsat 5 TM+ individual bands are composited into a single image using the Layer Stack function in ERDAS Imagine 9.3. After uncompressing all imagery and applying the layer stack function to the Landsat 5 TM+ imagery, these data must be set to a consistent projection before an Area of Interests (AOI) can be used to clip the images to the maximum extent of the study area.

When working with geospatial data it is important to ensure that all data are in the same projection before further geoprocessing takes place. Landsat 5 TM+ imagery has a parent projection of WGS 1984 UTM+ and MODIS MOD11A1 has a parent projection of Sinusoidal. The projection of UTM and a datum of WGS 1984 were selected as the standard for this study. In order to overlay MODIS MOD11A1 imagery with Landsat 5 TM+, MODIS MOD11A1 must first be projected to Geographic Coordinate System (GCS) WGS 1984, and then projected to WGS 1984 UTM+ Zone 16 for Indianapolis, IN. At this point images are aligned and projected in the same system and ready for further processing.

After normalizing each raster to the same projection an AOI can be defined to clip each image down to the maximum areal extent. To define the AOI for the raster clipping process 2000 Census County Shapefiles were used. The 2000 Census County Shapefile data were re-projected to WGS 1984 UTM for Indianapolis. The raster clipping tool in ArcInfo 10.0 was used to clip each raster to the maximum extent of each county boundary.

**Thermal Image Processing – Urban Heat Island Mapping**

The Landsat 5 TM+ and MODIS MOD11A1 sensors involve a degree of post processing to convert Top-Of-Atmosphere (TOA) radiances to LSTs. The MODIS MOD11A1 thermal data is delivered nearly complete for LST mapping and analysis while the Landsat 5 TM+ sensor requires more processing in order to obtain a LST value. The steps involved in converting TOA radiances to LSTs are described below. It is important to mention that at-sensor acquisition for each satellite is different. Emissivities are estimated from land cover types in MODIS MOD11A1 (NASA, 2011). Landsat 5TM+ records an at-sensor brightness value that is converted to an at-sensor brightness temperature by using constants published by Chander, Gyanesh., Markham, Brian L., and Helder, Dennis L (2009).

**LST Methodology for Landsat 5 TM+**

Chander et al. published a methods paper describing "equations and parameters to convert calibrated Digital Numbers (DNs), to physical units, such as at-sensor radiance or [TOA] reflectance" (2009). This paper "tabulates the necessary constants for all the Landsat sensors in one place" (Chandar et al., 2009). Chander et al. state, "converting at-sensor spectral radiance is a fundamental step in converting raw image data from multiple sources and platforms into a physically meaningful common radiometric scale" (2009). Essentially raw DNs are calibrated to Digital Numbers (Chander et al., 2009). In order for the DNs to be converted to a LST, "conversion of the at-sensor brightness temperature must take place" (Chander et al., 2009). The thermal band from Landsat sensors can be converted from at-sensor spectral radiance to effective at-sensor brightness temperature (Chander et al., 2009).

The authors note that "at-sensor brightness temperature assumes that the Earth's surface is a black body (i.e., spectral emissivity is 1), and includes atmospheric effects (absorption and emissions along a path)" (Chander et al., 2009). Chander et al. have provided "equations and rescaling factors for converting Landsat DNs to absolute units of at-sensor spectral radiance, TOA reflectance, and at-sensor brightness temperature" (2009). Their paper "tabulates the necessary constants for MSS, TM+, ETM+, and ALI sensors in a coherent manner using the same units and definitions" (Chander et al., 2009).

**LST Methodology for MODIS Terra / MOD11A1**

The initial value recorded by MOD11A1 is a top of atmosphere radiance (TOA) and requires minimal post processing. The digital number recorded for each pixel value in the delivered product reflects the coefficients of the calibration, which must be converted by the end-user to obtain a LST value (Wan, 2007). To do this a model was built in ERDAS Imagine 9.3

to multiply each pixel value by a scaling factor of 0.02 which converts the pixel value to Kelvin (Wan, 2007).

**Composite Downscaling Methodology**

Before downscaling can take place it is important that the data from both sensors be standardized. In this study LSTs for each image from both sensors have been converted to a Z-score. Converting observations to a Z-score is a meaningful way of measuring the number of standard deviations from the mean (Agresti and Finaly, 2009). To calculate a Z-score, observed values are subtracted from the mean, and then divided by the standard deviation of the observed values (Agresti and Finaly, 2009). The mean and standard deviation for each day of imagery can be found in Table 2, Image Statistics. To convert LST values to a Z-score the mean and standard deviation of all LSTs (Landsat 5 TM+ and MODIS) need to be tabulated (Table 2). These data were obtained through the ImageInfo window in ERDAS Imagine 9.3. Zero values were ignored when gathering image statistics.

When obtaining image statistics for remote sensor imagery it is important to consider how clouds are processed. For example in Landsat 5 TM+ clouds are not removed from the image. The pixels associated with clouds in Landsat 5 TM+ are cloud top temperatures. The temperatures associated with cloud tops are cooler than the LSTs surrounding the cloud covered areas. When gathering image statistics the lower LST values associated with the cloud tops can skew the mean LST and Standard deviation for the scene. MODIS MOD11A1 deals with cloud coverage in a different way. Pixels that are associated with cloud coverage in MODIS MOD11A1 are masked out and the pixel value is replaced with a no data value. No data values were selected to be ignored when gathering image statistics for MODIS MOD11A1 thermal imagery. This is done to give a more meaningful mean and standard deviation for pixels that have a LST value. MODIS MOD11A1 images that were at full or near full cloud coverage were discarded

and not used in downscaling. MODIS MOD11A1 images that have been discarded are documented in Table 2.

After converting LST values to Z-scores downscaling can begin to take place. Using the model builder in ERDAS Imagine 9.3, the Z-scores from the initial Landsat 5 TM+ thermal band are subtracted from Z-scores from the MODIS MOD11A1 thermal band from the same day, and combined into a new output image. Z-scores are reported in negative and positive integers. This is the initial downscale calibration for the first day of the sixteen day lapse until the next Landsat 5 TM+ scene.

Landsat 5 TM+ is subtracted from MODIS MOD11A1 rendering the initial downscale from both images identifying the values above and below the mean. The initial calibration image created between the same day's Landsat 5 TM+ and MODIS MOD11A1 thermal imagery are then added to the subsequent day's MODIS MOD11A1 scene. This gives a daily guidance as to whether specific areas of a city are getting warmer or cooler on a daily basis. Positive integers represent downscaled values that are warmer than the previous day's LST and negative integers represent values that are cooler than the previous day's LST. These steps represent the downscale of thermal imagery to Landsat 5 TM+ with the resulting output being a composite of LST values from both sensors on the same day. After the initial downscale of MODIS MOD11A1 to Landsat 5 TM+ resolutions the following day's MOD11A1 images are downscaled to the next cloud free Landsat 5 TM+ pass.

**Results and Future Considerations**

Testing of the above method was unsuccessful in statistically downscaling MODIS MOD11A1 thermal imagery to the spatial resolutions of Landsat 5 TM+ thermal imagery. Although testing of the composite downscale method was unsuccessful in calibrating daily MODIS MOD11A1 thermal bands to higher spatial resolution of Landsat 5 TM+, this study has been successful in identifying areas for future considerations, as well as provide a description of the challenges that should be considered if this method is to advance. The next section presents the Individual Downscale method, which should be considered for further evaluation.

The presence of clouds in remote sensing studies can often be problematic as was the case in this study. The time span in this study was seventeen days (2011-07-15 through 2011-07-31) which encompasses the time period between two Landsat 5 TM+ acquisitions. The proposed objective of this study was to create a daily-downscaled composite LST image until the next Landsat 5 TM+ acquisition. In order to validate the model error was going to be measured between the composite image (2011-07-15 through 2011-07-31) to the Landsat 5 TM+ image acquired on 2011-07-31. These tests were unable to be run due to difficulties posed by clouds / no data values in the model.

Table 3, Indianapolis Cloud Coverage shows cloud coverage in pixels and as a percent of cloud coverage for the study area. MODIS MOD11A1 scenes for Indianapolis, IN cover a pixel area of 25 by 25 which equals 625 available pixels for the AOI. Day one MODIS MOD11A1 for this study is the most cloud free with total percent cloud coverage at 6.08%, which equals 38 pixels with clouds (Table 3). Four MODIS MOD11A1 images were discarded due to total cloud coverage (Table 3) leaving thirteen days of MODIS MOD11A1 imagery to be downscaled up and to the next cloud free Landsat 5 TM+ pass. As seen in Table 3, during the thirteen day study period there are a total of 8125 pixels, 4407 have LST values, and 3781 are cloud pixels. A

possible work around for the cloud issue would be to discard all images that were grater than 50%. In the case of this study that would have eliminated seven of the thirteen usable images. When including the four days of total cloud coverage that totals eleven images from the seventeen day study period. After looking at these data from this perspective it might be beneficial to increase the temporality of this study to be able to include more samples.

The post processing of clouds in Landsat 5 TM+ and MODIS MOD11A1 thermal imagery is dealt with differently. In Landsat 5 TM+ clouds are not removed in post processing after at-sensor acquisition. The cloud top temperatures in Landsat 5 TM+ can have implications in statistical analysis due to the cloud tops being cooler than the surface temperatures. The scope of this study was not to research how to remove clouds from images, but it might be considered in the future for Landsat 5 TM+ images that have greater amounts of cloud coverage. In MODIS MOD11A1 thermal imagery clouds are removed and replaced with a no data value. The main issue in this study is in the difference of how each of these thermal images is post processed with respect to clouds. The no data value in MODIS MOD11A1 thermal imagery percolates an issue through the model which occurs during the initial calibration on day one between Landsat 5 TM+ and MODIS MOD11A1.

During day one calibration the most recent cloud free Landsat 5 TM+ image is subtracted from the same day of MODIS MOD11A1 thermal imagery. As mentioned above MODIS MOD11A1 thermal imagery replaces clouds pixels with a no data value. In the pilot study for this project it was discovered that in order to bring the Z-score value through from day one calibration to day two calibration MODIS MOD11A1 no value pixels need to be converted to zero. MODIS MOD11A1 thermal imagery was exported with no data values as zero using ArcInfo 10.0. Doing so replaces the no data value with zero, which eliminates issues when doing raster

calculations. Day two calibration can take place with the no data issue addressed, although other anomalies occur which are described below.

When subtracting Landsat 5 TM+ from MODIS MOD11A1 on day one a calibration is made for all areas where MODIS MOD11A1 has a Z-score. In the areas that contain zero values the Z-score value from the Landsat 5 TM+ image remains un-calibrated until there is a MODIS MOD11A1 scene that has a Z-score value where there was previously a cloud pixel. When the initial calibration image (day one) is added to day two, the cell values from the initial calibration percolate through doubling the cell value because an initial difference has not been able to be calculated for the MODIS MOD11A1 cells that had clouds on day one. The initial calibration was run using LST values instead of Z-scores to assess if the Z-scores were the issue. This generated the same results as with the Z-scores. LST values continue to nearly double as each day's MODIS MOD11A1 scene is added after the initial calibration. The minimum range for day one initial calibration in terms of LST is -15 Kelvin to 315 Kelvin. The minimum (-15 Kelvin) represents the difference of Landsat 5 TM+ from the same day's MODIS MOD11A1 scene where there are LST values. The maximum (315 Kelvin) is representative of the background values from Landsat 5 TM+ that have not been calibrated due to the zero value. The maximum value for day two nearly doubles (620 Kelvin). This is due to clouds being in the same place in MODIS MOD11A1 from day one and day two. As a simple test to try to circumvent the doubling effect each image was divided by two after each day's calibration. This did not work as it brought the minimum and maximums closer to zero after each day's calibration.

With the range issue at hand a cloud mask was generated for each MODIS MOD11A1 scene to try to circumvent the doubling of values in areas of cloud coverage from day one calibration. This was accomplished by running a conditional statement in ERDAS Imagine 9.3. In the conditional statement zeros which are clouds in the MOSIS imagery were turned into ones

and all other cells containing LST values were changed to zeros. The process of masking the clouds during downscaling works on the initial calibration, but not on the following day. The mask on the previous day does not account for areas were there might be cloud coverage the next day. The issue at hand here stems from the areas where there are clouds in MODIS MOD11A1 on day one initial calibration. As another mechanism to assess the nature of clouds in the MODIS MOD11A1 data an "or" statement was run in ERDAS Imagine 9.3 to assess the total number of pixels that were cloud free for the study period, and the result was two pixels in a 25 by 25 scene (625 pixels) over the period of thirteen images.

Something to be cautious about in the processing of these data are edge effects. Many times after analysis, even when using an AOI for analysis, values outside the AOI contain extremely large negative values. To work around this issue imagery in this study was clipped to the AOI and then exported using the method above in ArcInfo 10.0. This would correct the range of the data and prepare it for downscaling on the next day.

Something else to consider is exactly how ERDAS Imagine is making the calculations between a one-kilometer pixel (MODIS MOD11A1) and a 30-meter pixel (Landsat 5 TM+). There are approximately 1,109 Landsat 5 TM+ pixels that are downscaled to the one-kilometer pixel resolution of MODIS MOD11A1. If this study is carried forward is it highly recommended that the next researcher investigate how the programs are making these calculations.

As mentioned above Landsat 5 TM+ does not remove clouds in post processing. If this work is moved forward it would be worth considering testing thermal imagery from different sensors as an alternative to the MODIS sensor which does not remove clouds in post processing. A new issue may arise with values being skewed by the cooler temperatures of cloud tops, but this could be dealt with in a statistical manor.

Another concern is more logistical and would be relevant if this work is put into implementation. MODIS MOD11A1 thermal imagery is processed within approximately 24 hours of acquisition. If this method were to be put into implementation the thermal data from MODIS MOD11A1 would need to be processed into the heat wave vulnerability models within that 24 hour time period in order to calibrate the model with the new daily downscaled LST. MODIS MOD11A1 data are usually available for download from the GloVis site within five days of image acquisition. MODIS MOD11A1 imagery would need to be accessed and factored into the heat wave models as soon as available from NASA. This is important to keep in mind, as heat events are sometimes short in duration.

**Individual Downscaling Method**

Downscaling MODIS MOD11A1 to Landsat 5 TM+ on an individual basis opposed to creating a composite image appears to generate useable information that with further testing has potential to be incorporated into the Enhanced Heat Vulnerability Index (EHVI). The more important objective of this work was to generate a daily downscaled LST value using Landsat 5 TM+ and MODIS MOD11A1. Instead of creating a daily composite image from the previous days LST daily MODIS MOD11A1 can be downscaled on an individual basis circumventing the issues observed when compositing the image with the previous days downscaled image.

Subtracting Day 1 Landsat 5 TM+ from Day 2 MODIS MOD11A1 accomplishes the individual downscale. This results in a single composite image between Landsat 5 TM+ and MODIS MOD11A1. Downscaling MODIS MOD11A1 individually to Landsat 5 TM+ removes the issue of no data values and the doubling effect in MODIS MOD11A1. When subtracting day 1 (Landsat 5 TM+) from Day 2 (MODIS MOD11A1) a calibration takes place in the areas where there was not cloud coverage in the MODIS MOD11A1 image. Areas of cloud coverage remain at zero or remain at the prior calibration until that area is cloud free. These calibrated values could be inputted into the EHVI and re-ran with the downscaled LST values in order to model vulnerability for the next day. Calibrations would continue to take place based on day 1 Landsat 5 TM+ LST values until the next cloud free Landsat 5 TM+ pass. A measure of error would need to be identified before the individual downscaled calibrations were incorporated into the EHVI.

## Conclusion

This study shows proof of concept for the methodology tested and also provides insight as to where to direct this work in the future. With funding for the sciences becoming more limited at the present time it is important to use the information we have available today. The temporal resolution of the MODIS makes this sensor a great candidate to fuse with other remote sensor data that has higher spatial resolutions and less temporal coverage. It is strongly recommended that this study continue to a point of validation. This method not only has potential to calibrate the EHVI, but it could also be used as a tool to measure how different locations are warming and cooling in the urban environment during a heat wave.

APPENDIX A

Table 1: Selected Sensors for Study

| Thermal Infrared Sensors (TIR) | Spatial Resolution | Spectral Resolution | Temporal Resolution | Radiometric Resolution |
|---|---|---|---|---|
| *Landsat 5 TM+ (Thematic Mapper)* | 120 M x 120 M | Band 6<br>10.40µ - 12.50µ | 16 Days | 8 bit |
| *MODIS Terra (Moderate Resolution Imaging Spectroradiometer)* | 1 KM x 1KM | Band 31<br>10.780µ - 11.280µ<br>Band 32<br>11.770µ - 12.270µ | Twice Daily | 16 bit unsigned |

Table 2: Image Statistics

| Landsat 5 TM+ | | |
|---|---|---|
| **Date** | **STDEV** | **Mean** |
| 2011-07-15 | 13.14 | 300.86 |
| 2011-07-31 | 3.93 | 300.88 |
| **MODIS MOD11A1** | | |
| **Date** | **STDEV** | **Mean** |
| 2011-07-15 | 2.28 | 301.46 |
| 2011-07-16 | 2.18 | 305.67 |
| 2011-07-17 | 1.66 | 299.76 |
| 2011-07-19 | 1.39 | 303.17 |
| 2011-07-21 | 2.22 | 308.99 |
| 2011-07-22 | 0.78 | 300.30 |
| 2011-07-23 | 2.08 | 304.58 |
| 2011-07-25 | 2.17 | 303.32 |
| 2011-07-26 | 1.68 | 300.84 |
| 2011-07-27 | 2.07 | 303.09 |
| 2011-07-28 | 3.95 | 301.53 |
| 2011-07-30 | 2.10 | 305.21 |
| 2011-07-31 | 1.29 | 302.26 |

Table 3: Indianapolis MODIS Cloud Coverage

| Columns / Rows 25x25 (625) | | | | |
|---|---|---|---|---|
| **Date** | **Total Pixels** | **Pixels with LST** | **Cloud Pixels** | **Total % CC** |
| 2011-07-15 | 625 | 587 | 38 | 6.08% |
| 2011-07-16 | 625 | 303 | 322 | 51.52% |
| 2011-07-17 | 625 | 181 | 444 | 71.04% |
| 2011-07-18 | 625 | 0 | 625 | 100.00% |
| 2011-07-19 | 625 | 289 | 336 | 53.76% |
| 2011-07-20 | 625 | 0 | 625 | 100.00% |
| 2011-07-21 | 625 | 552 | 73 | 11.68% |
| 2011-07-22 | 625 | 66 | 559 | 89.44% |
| 2011-07-23 | 625 | 320 | 305 | 48.80% |
| 2011-07-24 | 625 | 0 | 625 | 100.00% |
| 2011-07-25 | 625 | 386 | 239 | 38.24% |
| 2011-07-26 | 625 | 243 | 382 | 61.12% |
| 2011-07-27 | 625 | 297 | 328 | 52.48% |
| 2011-07-28 | 625 | 251 | 374 | 59.84% |
| 2011-07-29 | 625 | 0 | 625 | 100.00% |
| 2011-07-30 | 625 | 553 | 72 | 11.52% |
| 2011-07-31 | 625 | 379 | 246 | 39.36% |
| Pixel Totals | 10625 | 4407 | 6218 | |

APPENDIX B

Figure 1: MODIS MOD11A1 Downscaling Equation

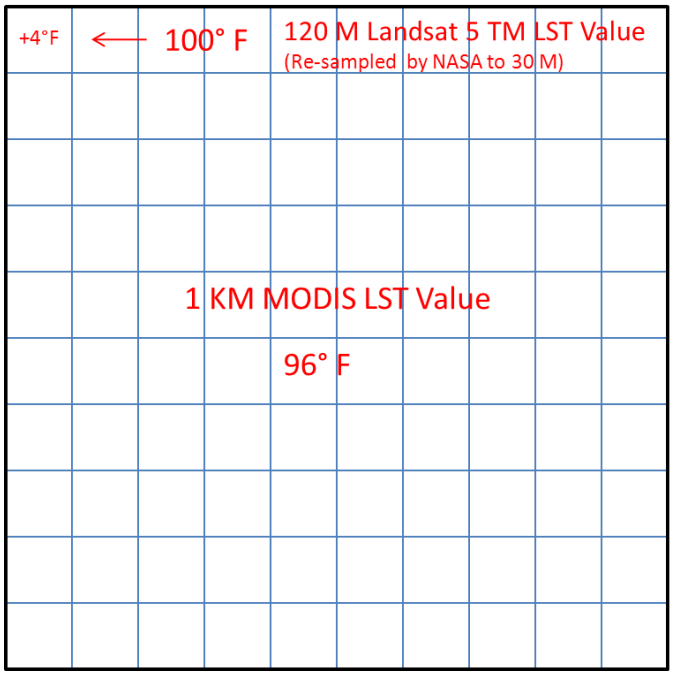


$$T_M \approx \sum WT_{TM}(n)$$

**Where:**

$T_M$= MODIS LST

W = $T_M$ + or - $T_{TM}$

$WT_{TM}$= (Weighted LST Value)

n = MODIS Matrix ($10_{60\,M}$ x $10_{60\,M}$)

$T_M$ approximates the sum of $T_{TM}$

REFERENCES

Agresti, Alan, & Finlay, Barbara. (2009). Statistical Methods for the Social Sciences. Lynch (Ed.), (Fourth ed.). Upper Saddle River: Pearson.

Alley, Richard, Berntsen, Terje, Bindoff, Nathaniel L., Chen, Zhenlin, Chidthaisong, Amnat, & et al. (2007). Climate Change 2007: The Physical Science Basis Summary for Policymakers IPCC WGI Fourth Assessment Report (pp. 1-21). Geneva, Switzerland.

Bernard, Susan M., & McGeehin, Michael A. (2004). Municipal Heat Wave Response Plans. American Journal of Public Health, 94(9), 1520-1522.

Cakir, Halil I., & Khorram, Siamak. (2008). Pixel Level Fusion of Panchromatic and Multispectral Images Based on Correspondence Analysis. Photogrammetric Engineering & Remote Sensing, 74(2), 183-192.

Centers for Disease Control. (2001). Heat-Related Deaths --- Los Angeles County, California, 1999--2000, and United States, 1979--1998. MMMR Weekly, 50(29), 623-626. http://www.cdc.gov/mmwr/preview/mmwrhtml/mm5029a3.htm

Centers for Disease Control. (2002). Heat-Related Deaths --- Four States, July--August 2001, and United States, 1979--1999. MMMR Weekly, 51(26), 567-570. http://www.cdc.gov/mmwr/preview/mmwrhtml/mm5126a2.htm

Centers for Disease Control. (2004). Extreme Heat Fact Sheet. 2. http://www.bt.cdc.gov/disasters/extremeheat/pdf/elderlyheat.pdf

Chandar, Gyanesh, Markham, Brian L., & Helder, Dennis L. (2009). Summary of current radiometric calibration coefficients for Landsat MSS, TM, ETM+, and EO-1 ALI sensors. Remote Sensing of Environment, 113, 893-903.

Cutter, Susan L., Boruff, Bryan J., & Shirley, W. Lynn. (2003). Social Vulnerability to Environmental Hazards. Social Science Quarterly, 84(2).

Dong, Jiang, Zhuang, Dafang, Huang, Yaohuan, & Fu, Jingying. (2009). Advances in Multi-Sensor Data Fusion: Algorithms and Applications. Sensors, 9.

Environmental Protection Agency. (2006). Excessive Heat Events Guidebook. Washington D.C.: United States Government.

ERDAS Imagine. (2009). ERDAS Field Guide. Norcross: ERDAS, Inc.

Jensen, John R. (2005). Introductory Remote Sensing - A Remote Sensing Perspective (3 ed.). Upper Saddle River: Pearson - Prentice Hall.

Johnson, Dan, Lulla, Vijay, Stanforth, Austin, & Webber, Jeremy. (2011). Remote Sensing of Heat-Related Health Risk: The Trend Toward Coupling Socioeconomic and Remotely Sensed Data. Geography Compass, 5(10), 767-780.

Johnson, Daniel P., & Wilson, Jeffrey S. (2009). The socio-spatial dynamics of extreme urban heat events: The case of heat-related deaths in Philadelphia. Applied Geography (29), 419-434.

Johnson, Daniel P., Wilson, Jeffrey S., & Luber, George C. (2009). Socioeconomic indicators of heat-related health risk supplemented with remotely sensed data. International Journal of Health Geographics, 8(57).

Karl, Thomas R., Melillo, Jerry M., & Peterson, Thomas C. (2009). Global Climate Change Impacts in the United States.

Luber, George, & McGeehin, Michael. (2008). Climate Change and Extreme Heat Events. American Journal of Preventive Medicine, 35(5), 429-435.

National Aeronautics and Space Administration. (2012). Earth Observing System Data and Information System FAQ. Retrieved 07/02/2012, 2012, from http://earthdata.nasa.gov/data/nrt-data/help/faq

National Aeronautics and Space Administration, Land Processes Distribution Active Archive Center. (2010). Land Surface Temperature and Emissivity Daily L3 Global 1 km Grid SIN MOD11A1. Retrieved 07/06/2012, 2012, from https://lpdaac.usgs.gov/products/modis_products_table/land_surface_temperature_emissivity/daily_l3_global_1km/mod11a1

National Weather Service. (2011). Heat: A Major Killer. Retrieved 08/08/11, 2011, from http://www.nws.noaa.gov/om/heat/index.shtml

Pengelly, L. David, Campbell, Monica E., Cheng, Chad S., Fu, Chao, Gingrich, Sarah E., & Macfarlane, Ronald. (2007). Anatomy of Heat Waves and Mortality in Toronto: Lessons for Public Health Protection. Canadian Journal of Public Health-Revue Canadienne De Sante Publique, 98(5), 364-368.

Robinson, Peter J. (2000). On the Definition of a Heat Wave. Journal of Applied Meteorology, 40.

Sheridan, Scott C. (2006). A survey of public perception and response to heat warnings across four North American cities: an evaluation of municipal effectiveness. International Journal of Biometeorology, 52(3), 3-15.

Simone, G., Farina, A., Morabito, F.C., Serpico, S.B., & Bruzzone, L. (2001). Image fusion techniques for remote sensing applications. Information Fusion, 3(15), 3-15.

Stone, Brian, Hess, Jeremy J., & Frumkin, Howard. (2010). Urban Form and Extreme Heat Events: Are Sprawling Cities More Vulnerable to Climate Change Than Compact Cities? Environmental Health Perspectives, 118, 1425-1428.

United States Geological Survey, Earth Explorer. (2009). Landsat Product Type Descriptions. Retrieved 05-16-12, 2011, from http://edcsns17.cr.usgs.gov/helpdocs/landsat/product_descriptions.html#terrain_l5_l1t

WTHR Channel 13. (2011). Indianapolis opens cooling centers during heat wave. Retrieved 11/29/2011, from http://www.wthr.com/story/15101173/indianapolis-may-open-cooling-centers-during-heat-wave

Zhengming, Wan. (2007). Collection-5 MODIS Land Surface Temperature Products Users Guide. 60. http://www.icess.ucsb.edu/modis/LstUsrGuide/MODIS_LST_products_Users_guide_C5.pdf

CURRICULUM VITAE

J. Jeremy Webber III

**Education**

Indiana University, Indianapolis, IN

- Master of Science, August 2013, Geographic Information Science (MS GISci)
- Graduate Certificate in Geographic Information Science, December 2008
- Bachelor of Arts in Physical Geography, Geology Minor, Anthropology Minor, August 2006

**Experience**

Research Scientist – Remote Sensing and GIS Specialist, Center for Earth and Environmental Science (CEES), Department of Earth Sciences - IUPUI, Indianapolis, IN

*May 2012 – Present*

Indiana's Fluvial Erosion Hazard Mapping (FEH) Project

- Current work focuses on developing a semi-automated method using in situ and remote sensor data to predict meander belt width frequency in fluvial systems.
- Researching and developing a data fusion approach to access the sensitivity of FEH in different physiographic regions of Indiana through the use of in situ and remote sensor data.

Adjunct Instructor, Indiana University Purdue University Indianapolis - IUPUI, Indianapolis, IN

*January 2013 – May 2013*

- Weather and Climate – G303 (Spring 2013)

Research Associate, Department of Geography - IUPUI, Indianapolis, IN

*January 2010 – August 2012*

National Aeronautics and Space Administration (NASA) Research Opportunities in the Space and Earth Sciences (ROSES) Grant

- Work focused on developing methods to help predict spatial patterns of morbidity and mortality associated with extreme heat events in urban areas.
- Researched and developed a method for statistically downscaling MODIS Thermal Imagery to Landsat 5 TM+ Resolutions.

Adjunct Instructor, Indiana University Purdue University Columbus - IUPUC, Columbus, IN

*January 2010 – May 2012*

- Introduction to Physical Geography – G107 (Spring 2010, Fall 2010, Spring 2011, Fall 2011, and Spring 2012)
- Introduction to Human Geography – G110 (Spring 2011, Fall 2011, and Spring 2012)

Cartographer, Center for Earth and Environmental Science (CEES), Department of Earth Sciences - IUPUI, Indianapolis, IN

*May 2008 – December 2009*

Grant based projects:

- USDA Conservation Effects Assessment Project (CEAP) - Eagle Creek Watershed, Indiana.
  Visual interpretation of conservation buffers and land use features.
  Developed drainage networks and runoff models using high resolution elevation data.

- Lake and River Enhancement Grant (LARE) - Indiana Department of Natural Resources (DNR) Upper White River Watershed, Indiana.
  Created an atlas of static maps relating to water quality for the Upper White River Watershed.

Graduate Research Assistant, Department of Geography - IUPUI, Indianapolis, IN
*September 2006 – May 2008*

- Used high resolution geospatial data for land use characterizations and surface hydrology modeling. Graduate course work focused towards environmental applications of GIS and remote sensing.
- Water quality data analysis and visualization.
- Tutored Physical Geography students to help develop or expand their quantitative skills.

Undergraduate Research Assistant, Center for Earth and Environmental Science (CEES) - IUPUI, Indianapolis, IN
*September 2004 – August 2006*

- Assisted in various aspects of watershed monitoring and ecosystem restoration in Central Indiana watersheds. Work involved soil characterization, surveying stream cross-sections, and water quality monitoring and analysis, which developed field methods and quantitative skills.
- Responsible for cartography and GIS projects ranging from data collection, processing, analysis, and thematic design.
- Participated in environmental outreach programs for K-12 audiences.

Service Learning Intern, Center for Earth and Environmental Science (CEES) - IUPUI, Indianapolis, IN
*September 2002 – August 2004*

- Promoted land stewardship through experiential environmental based service projects.
- Responsible for leading service learning projects and teaching environmental science workshops to K-12, college students, and teachers.
- Environmental monitoring; lake, stream, and groundwater.

**Publications and Presentations**

Using LiDAR to Improve Fluvial Erosion Hazard Mapping, J. Jeremy Webber and Robert Barr. 2013 Indiana GIS Conference. Muncie, IN, May 7th, 2013. (Presentation)

Spatiotemporal Variations in Heat-Related Health Risk in Three Midwestern U.S. Cities Between 1990 and 2010, Daniel P. Johnson Ph.D., J. Jeremy Webber M.S., Kavya Urs Beerval Ravichandra M.S., Vijay Lulla Ph.D., and Austin C. Stanforth M.S. Geocarto International: In press (Paper)

Lessons Learned on Keeping Soil, Nutrients, and water in your fields, Barr, R.C., Stouder, M.D., and Webber, J. 2013 National No-Till Conference. Indianapolis, IN, Jan 11, 2013. (Presentation)

Northwest Indiana Regional FEH Workshop, Barr, R.C., Robinson, B. A., Stouder, M.D., and Webber, J. Indiana Silver Jackets. Sponsored by the Maumee River Basin Commission. Auburn, IN. Nov 20, 2012. (Presentation)

Southeast Indiana Regional FEH Workshop, Barr, R.C. Robinson, B. A., Stouder, M.D., and Webber, J. Indiana Silver Jackets. Sponsored by the Historic Hoosier Hills RC&D. Clifty Falls State Park, Madison, IN. Nov 15, 2012. (Presentation)

Northwest Indiana Regional FEH Workshop, Barr, R.C., Robinson, B. A., Stouder, M.D., and Webber, J. Indiana Silver Jackets. Sponsored by the Kankakee River Basin Commission. Portage, IN. Nov 13, 2012. (Presentation)

Southwest Indiana Regional FEH Workshop, Barr, R.C., Robinson, B.A., and Webber, J. Indiana Silver Jackets. Sponsored by the Southwest Indiana Watershed Alliance and Vincennes University. Vincennes University, Vincennes, IN, Nov 8, 2012. (Presentation)

Central Indiana Regional FEH Workshop, Barr, R.C., Robinson, B.A., and Webber, J. Indiana Silver Jackets. Sponsored by the Indiana Watershed Leadership Academy, Purdue University. West Lafayette, IN. Nov 1, 2012. (Presentation)

The Indiana Fluvial Erosion Hazard Mitigation Program, Barr, R.C., Cummins, J., Riggs, M., Robinson, B.A., Stipe, V., Stouder, M.D., and Webber, J. Indiana Association for Floodplain and Stormwater Management, Fall Conference. Brown County State Park, Nashville, IN. September 14, 2012. (Presentation)

The Indiana Fluvial Erosion Hazard Mitigation Program, Barr, R.C., Cummins, J., Riggs, M., Robinson, B.A., Stipe, V., Stouder, M.D., and Webber, J Association of Indiana Counties Annual Meeting. Indianapolis, IN, September 24, 2012. (Presentation)

The Indiana Fluvial Erosion Hazard Mitigation Program, Barr, R.C., Cummins, J., Riggs, M., Robinson, B.A., Stipe, V., Stouder, M.D., and Webber, J. KAMM Conference, Kentucky Association of Mitigation Managers. Kentucky Lake, KY. September 20, 2012. (Presentation)

The Indiana Fluvial Erosion Hazard Mitigation Program, Barr, R.C., Cummins, J., Riggs, M., Robinson, B.A., Stipe, V., Stouder, M.D., and Webber, J. Indiana Association for Floodplain and Stormwater Management, Fall Conference. Brown County State Park, Nashville, IN. September 14, 2012. (Presentation)

Using LiDAR to Reconstruct Historic Waterways of Indianapolis, Keep Indianapolis Beautiful Steering Committee Meeting
Pamela Martin PhD, J. Jeremy Webber, Indianapolis IN. August 2012 (Presentation)

The Indiana Fluvial Erosion Hazard Mitigation Program, Barr, R.C., Riggs, M., Robinson, B.A., Stouder, M.D., and Webber, J., Indiana Department of Natural Resources, Conservation and Natural Resource Engineering Continuing Education. Indianapolis, IN, June 12, 2012. (Presentation)

The State of the Oceans – Great Decisions Series, J. Jeremy Webber, Indiana University - Purdue University Columbus, Columbus, IN. March 2012 (Presentation & Moderator)

Remote Sensing of Heat-Related Health Risk: The Trend toward Coupling Socioeconomic and Remotely Sensed Data, Dan Johnson, Vijay Lulla, Austin Stanforth, Jeremy Webber. Geography Compass 5 10 (2011): 767-80. October, 2011 (Print)

Using NASA Data and Models to Improve Heat Watch / Warning Systems for Decision Support, Daniel P. Johnson PhD, Vijay Lulla PhD, J. Jeremy Webber, NASA Public Health Review, 2011 Santa Fe New Mexico September, 2011 (Presentation)

Modeling Vulnerability to Extreme Heat Events (EHE) Using Inputs from Remote Sensing and Socioeconomic Data, J. Jeremy Webber, Michelle Rigg, Daniel P. Johnson PhD. Department of Geography, IUPUI. The 22rd Annual Joseph Taylor Symposium, The Campus for the Community, February 2011, IUPUI Campus Center (Poster)

CEAP Watershed-scale Evaluation of BMP Effectiveness and Acceptability: Eagle Creek Watershed Indiana: 2009, Turco, R., Tedesco, L.P., Prokopy, L., Wilson, J., Frankenberger, J., Shively, J., Pascual, D., Arabi, M., Oliver, A., Weinkauf, D., Spencer, A., Hall, B., Barr, R., and Webber, J., 2009, USDA CSREES National Water Conference, St. Louis, 2009 (Presentation)

Watershed-Scale Evaluation of BMP Effectiveness and Acceptability: Eagle Creek Watershed, Turco, R., Tedesco, L., Prokopy, L., Wilson, J., Frankenberger, J., Shively, D., Pascual, D., Arabi, M., Weinkauf, D., Walker, B., Spencer A., Hall, B., Barr, R., and Webber, J., 2008, Indiana: United States Department of Agriculture Cooperative State Research, Education, and Extension Service 2008 National Water Conference, 2008 (Presentation)

The Development of Drainage Networks and Runoff Modeling – Central Indiana Watersheds, Indiana University, J. Webber, J. Wilson, B. Hall, R.C. Barr, L.P. Tedesco, April 2008, Indianapolis: Veolia Spring Science Meeting - Central Indiana Water Resource Partnership. (Presentation)

Using High Resolution Digital Surface Models to Evaluate and Manage the Impact of Urbanization on Primary Headwater Streams and Isolated Wetlands at Ritchey Woods Natural Area, Hamilton County, Indiana, J. Webber, R.C. Barr, B. Hall, L.P. Tedesco, May 2007, Terra Haute: American Society of Photogrammetry and Remote Sensing (ASPRS). (Presentation)

The impact of urbanization on basin evolution and isolated wetlands: A study from the Ritchey Woods Natural Area, Barr, R.C., Hall, B.E., Tedesco, L.P., Webber, J.J., and Hernly, F.V., 2005, Hamilton County, Indiana: Geological Society of America Abstracts with Programs, v. 37, no. 5, p.9. (Presentation)

Preserving “isolated” wetlands in evolving drainage basins: A study from the Ritchey Woods Natural Area Hamilton County, Indiana, Tedesco, L.P., Barr, R.C., Hall, B.E., Webber, J.J., and Hernly, F.V., 2005, Restoration and Design of Ecosystems, 5th Annual Meeting American Ecological Engineering Society Abstracts, p. 39. (Presentation)

Characterization of Wetland Soil and Sediments at Scott Starling Nature Preserve, Marion County, J. Jeremy Webber, F. Vincent Hernly, Lenore P. Tedesco, Bob E. Hall, April 2004: National Conference on Undergraduate Research National Conference, Indianapolis. (Presentation)

Characterization of Wetland Soil and Sediments at Scott Starling Nature Preserve, Marion County, Indiana University, J. Jeremy Webber, F. Vincent Hernly, Lenore P. Tedesco, Kara A. Salazar, Bob E. Hall; IUPUI Geology Department, 723 West Michigan Street, Indianapolis, Indiana 46202, November 2003: Geological Society of American Annual National Meeting in Seattle. (Presentation)

**Awards and Scholarships**

- NASA Research Opportunities in Space and Earth Sciences (ROSES) (2010-2012) Fellowship Recipient
- William M. Plater Award for Civic Engagement - Awarded to the top ten seniors who demonstrate both depth and diversity of commitment in serving their communities (2006)
- Carl M. Johnson Award - Awarded for scholastic achievement (2005)
- CEES Engaged Scholar - Funding for Undergraduate Summer Internship at CEES (2004)
- Sam H. Jones Scholarship - Funding for Undergraduate Service Learning Internship (2002 & 2003)

**Activities**

- Casting for Recovery Fly Fishing Instructor - Participate in teaching breast cancer survivors how to fly fish (2006-Present)
- The Hearth at Windermere: Presentation, Extreme Weather in Indiana (May, 2012)
- EPA Care Grant - Marion County Health Department (MCHD) & IU School of Public and Environmental Affairs (SPEA), Martindale Brightwood Community Project: Spatial analysis and data visualization (Spring 2009)
- Upper White River Watershed Alliance (UWRWA), 2007 - 2009 (Board Member May 2008-2009)
- Indiana Geographic Information Council (IGIC) Education Outreach Committee (2006-2008)
- Science Fair Judge - Jewell Christian Academy (2007 & 2009)
- Indiana Geographic Information Council (IGIC) Education / Outreach Committee Participant- Help develop and present professional education seminars (2007)
  - Surface Hydrology Modeling Seminar - Using GIS to Identify and Understand Wetlands,
    August 17, 2007
    Cartography Webinar - Making More Visually Pleasing Maps: Applied Cartography and Visualization,
    September 13, 2007
- Eiteljorg Museum Volunteer - Acted as an event coordinator and conducted independent research with IUPUI Faculty through the IUPUI - Eiteljorg Partnership (Fall 2006-Spring 2007). Presented Board of Directors with new events that were accepted and held during the Indian Market & Festival.